Accurate equivalent-network modelling of GaAs/AlAs based resonant tunnelling diode with symmetric thin barrier and spacer layers

Accurate Equivalent-Network Modelling of GaAs/AlAs Based Resonant Tunnelling Diodes with Symmetric Thin Barrier and Spacer Layers

J.J.M. Kwaspen, M.I. Lepsa[1], Th.G. van de Roer, H.C. Heyker, L.M.F. Kaufmann
Eindhoven University of Technology, Faculty of Electrical Engineering
COBRA Inter-University Research Institute on Communication Technology
Electronic Devices Group (TTE/EEA),
P.O. Box 513, NL-5600 MB Eindhoven, The Netherlands
Phone:+31 (0)40 - 247 5133 Fax: +31 (0)40 - 244 8375
E-mail: j.j.m.kwaspen@ele.tue.nl

Abstract—**On stable non-oscillating GaAs/AlAs based resonant tunnelling diodes with thin barriers, small-signal intrinsic impedances were measured at 21 °C in the full bias/frequency space (0-2V; 0.05-40.05 GHz). Equivalent-network optimisations for CAD, show that the classical Esaki model needs an extra degree of freedom for matching the measured intrinsic impedance throughout the whole active region. A very good impedance description in the entire bias/frequency space is obtained with four, frequency-independent intrinsic elements in the Quantum-Inductance model. Quasibound-state lifetime information and resistive cutoff-frequency, both against bias-voltage are shown.**

Keywords— **Resonant tunnelling diodes, equivalent-network modelling, compound semiconductors**

I. Introduction

With the accent on accuracy and full bias-voltage/microwave frequency range coverage (0-2V; 0.05-40.05 GHz), the classical Esaki and the Quantum Inductance (QI) equivalent-network models [1,2,3] are used here to describe the measured small-signal intrinsic impedance Z_d of our Double Barrier Resonant Tunnelling diodes (RTDs) for CAD purposes. The GaAs/AlAs based, MBE-grown devices have a 5 nm quantum well and symmetric thin barrier and spacer layers, each nominal 2.5 nm thick (Fig. 1).

The RTDs are of planar type, with coplanar microwave probe access from the network analyser to the metallised signal (SIG) and ground (GND) pads on the semi-insulating substrate (Fig. 2a). The DC I-V curve and the microwave reflection coefficient S_{11} of the extrinsic RTD, and S_{11} of an OPEN and a SHORT reference structure are measured at the reference planes (pads) indicated. The

[1] Permanent address: National Research Inst. for Material Physics, P.O.Box Mg-7 Magurele, 76900 Bucharest, Romania.

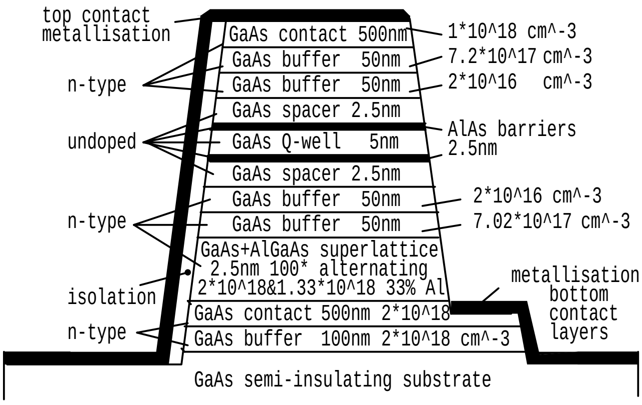

Fig. 1. RTD layer structure grown by molecular beam epitaxy (MBE); mesa definition by wet chemical etching; metallisation by lift-off technique; ohmic contacts Ge/Ni/Au; interconnections Ti/Pt/Au; isolation mesa-edge by SiO_2 or airbridge.

SHORT (Z_d = 0) and OPEN ($Z_d \Rightarrow \infty$) structures on the wafer (Fig. 2b,c) enable us to model the bias-voltage independent extrinsic elements of the equivalent-circuits: C_{ex}, R_{ex} and L_{ex} (Fig. 3), describing the microwave behaviour of the Ti/Pt/Au pads-to-mesa interconnections [6,7]. Only R_{ex} is frequency-dependent due to skin losses in the metallisation.

II. Stability Conditions and Measurements

Accurate determination of the actual intrinsic elements R_d (dynamic device resistance), C_d (dynamic device capacitance), L_q (quantum inductance) and R_s (series resistance), makes a stable, non-oscillating RTD in the negative differential resistance (NDR) region a prerequisite. A stable RTD has at least no chair-like plateaus in the NDR region of its I-V curve, so the conductance $G_d(= 1/R_d)$ has only one negative peak there (Fig. 4a,b). By proper

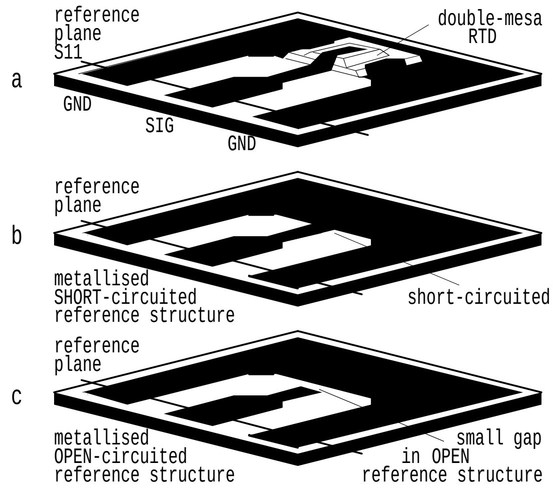

Fig. 2. (a) Planar RTD with coplanar probe access. (b) SHORT-reference structure $(Z_d = 0)$ (c) OPEN-reference structure $(Z_d \Rightarrow \infty)$

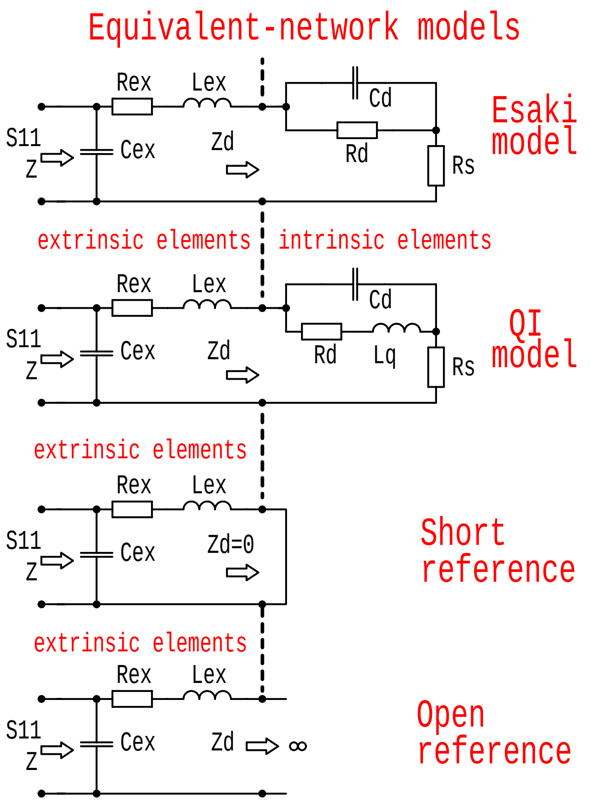

Fig. 3. Equivalent-circuit models of extrinsic RTD, consisting of interconnection elements Cex, Rex, Lex (pads-to-mesa), and intrinsic RTD equivalent-circuits: Esaki-model and Quantum Inductance (QI)-model. Also shown are the SHORT and OPEN reference structures.

choice of the device area (20 μm^2; to make $R_d + R_s + R_{ex}$ more negative than -50 Ω at the steepest slope in the NDR region, which gives a finite S_{11}) and a specially designed bias circuit, the stability condition was met in our experiments.

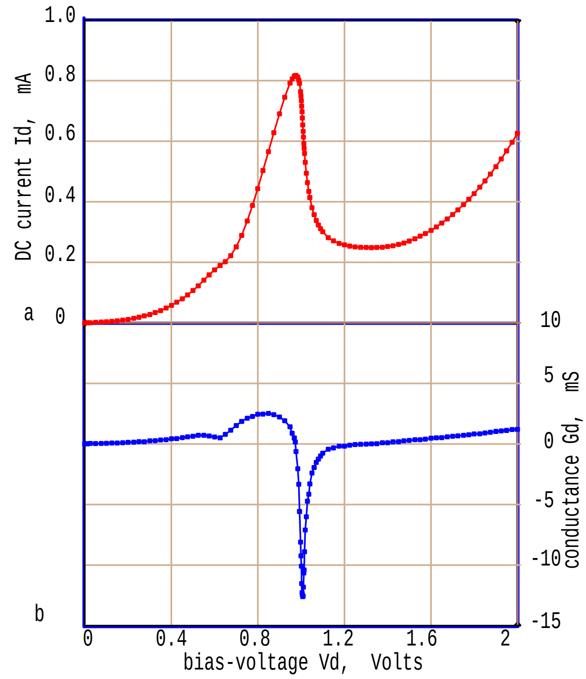

Fig. 4. (a) DC I-V curve of extrinsic RTD, measured at 21 °C (on-wafer reference plane). (b) Differential conductance Gd [mS].

An array of S_{11}-data was collected in the 0 to +2 V range of the I-V curve (mesa top is +V), where S_{11} of the extrinsic RTD was measured at 75 bias points and from 0.05 - 40.05 GHz (401 points), after network analyser calibration with on-wafer standards. Fig. 5 shows some of these S_{11}'s in a compressed Smith chart, amongst them S_{11} in the smallest-NDR point $(V_d = 1.0060V; |S_{11}| \sim 3.9)$. The prober-chuck temperature was 21 °C.

III. Esaki and Modified Esaki Models

Note that in a substantial range of NDR-region bias-voltages, the S_{11} curves show an inflection point, a feature that cannot be modeled by the Esaki equivalent-circuit with three, frequency-independent intrinsic elements (Fig. 3). Optimisation of these intrinsic parameters to carefully match the measured S_{11}-data (at each bias point), leads to the conclusion that the Esaki-model needs an extra degree of freedom to fit the measured S_{11} data array in the NDR region sufficiently accurate. Fig. 6a displays the real and imaginary parts of the intrinsic impedance Z_d at V_d = 1.0060 V (largest negative G_d), and Fig. 6b shows the dynamic conductance G_d and capacitance C_d, when these elements are taken frequency-dependent (in accordance with [4]) to match the measured S_{11}. The mathematical equations that describe G_d and C_d as a function of frequency in the modified Esaki-model are also bias-dependent, which complicates CAD use.

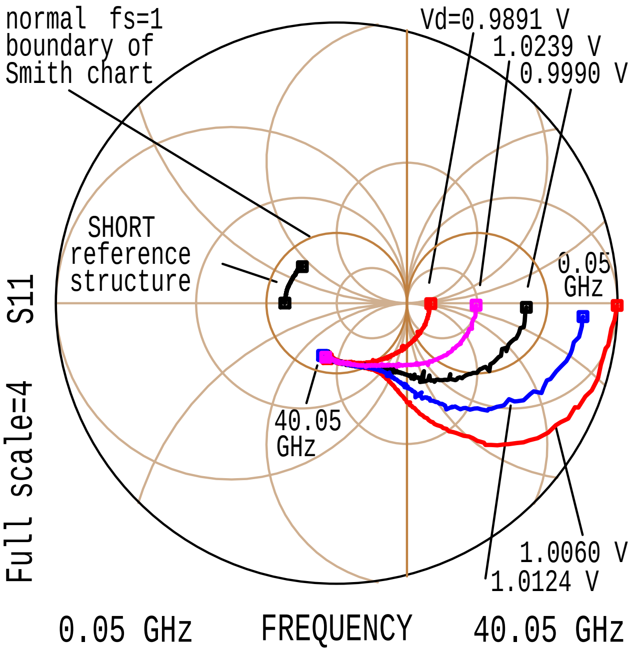

Fig. 5. Measured S_{11} of SHORT-reference $(Z_d = 0)$ and measured S_{11} of extrinsic RTD at several bias-voltages V_d, plotted in a compressed Smith chart (full scale= 4.0). Tchuck=21 °C.

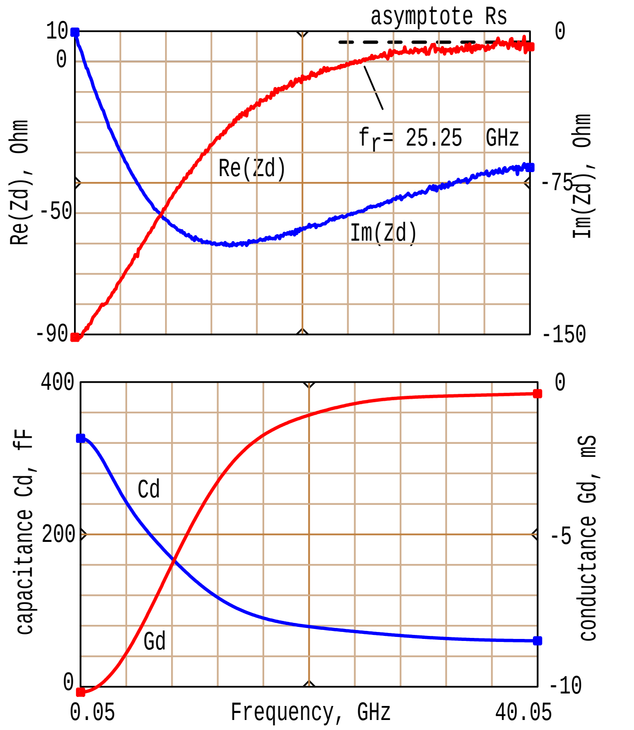

Fig. 6. (a) Real and imaginary parts of measured intrinsic RTD impedance Z_d, at steepest slope of NDR region (1.0060V). (b) Frequency-dependence of optimized dynamic elements C_d and G_d of modified Esaki-model (1.0060V).

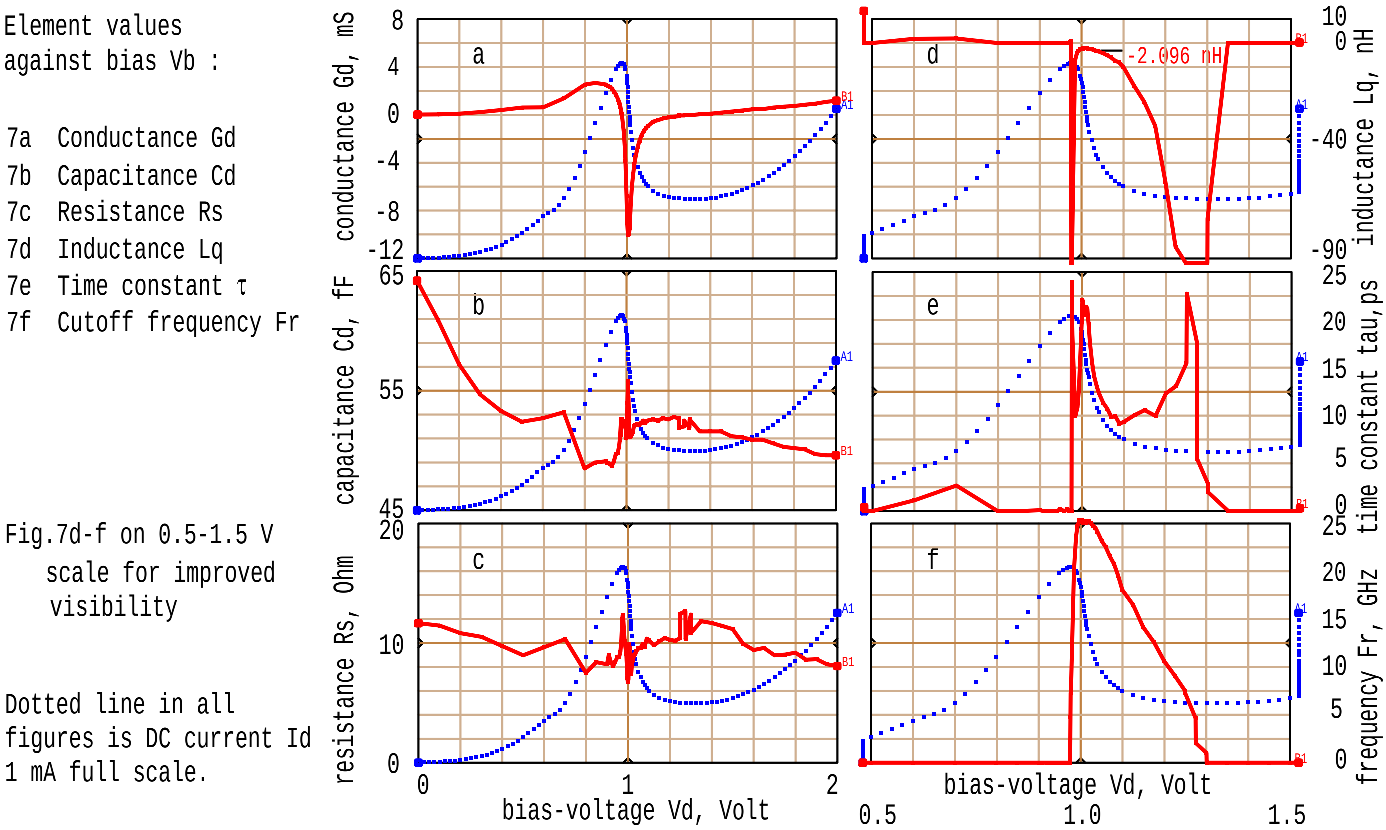

Fig. 7. Optimized intrinsic RTD elements Quantum Inductance (QI) model. Dynamic elements against bias-voltage, 75 points.

IV. Quantum Inductance Model

The same measured small-signal S_{11} datasets can be described 'perfectly' by the Quantum Inductance circuit model (Fig. 3) over the full bias-voltage (0-2 V) and frequency ranges (0.05-40.05 GHz) with four, frequency-independent intrinsic elements (Fig. 7a-d). The measurement of S_{11} on the stable RTD throughout the entire NDR region without hiatus, results in the correct determination of a time constant τ, here defined as $\tau = L_q/R_d (= L_q \cdot G_d)$ which, according to several authors [1,2], should be an indication of the quasibound-state lifetime in the quantum well. The display of this parameter τ (Fig. 7e) and of L_q continuously over the whole undistorted NDR region is a novelty. Near the point where G_d has zero conductance (at the peak and valley voltages), the values of τ are less reliable. τ is not defined where $G_d = 0$. The peak value of τ corresponds with the negative G_d-peak (same bias). The calculated quasibound ground-state lifetime τ_1 given in [5] of $\sim$ 50 ps for an AlAs barrier thickness of 2.547 nm and $\sim$ 18 ps for 2.264 nm (a decrease of 1 monolayer), compares well with the time constant τ = 22 ps measured. Fig. 7f shows the resistive cut-off frequency f_r against bias-voltage of the intrinsic RTD. In the passive regions of the I-V curve, the QI-model reduces to the Esaki-model, since the element-optimisation process finds there low values of L_q. For CAD purposes, a very good RTD intrinsic impedance description in the entire bias/frequency space (0-2V; 0.05-40.05 GHz) is obtained with four frequency-independent intrinsic elements, scalable with device area.

References

[1] E.R. Brown, et al, Appl. Phys. Lett., Vol. 54, (10), March 1989, pp. 934-936.

[2] O. Vanbesien, et al, Microwave and Opt. Techn. Lett., Vol. 5, (8), 1992, pp. 351-354.

[3] H.J.M.F. Noteborn, Ph. D.-thesis, Eindhoven University of Technology, Netherlands, May 1993.

[4] J. Genoe, Ph. D.-thesis, Catholic University of Leuven, Belgium, 1994.

[5] H. Brugger, et al, Proc. 18th Int. Symp. GaAs and Related Compounds, Seattle, Sept. 1991.

[6] J.J.M. Kwaspen, et al, WOCSDICE'97, May 1997, Scheveningen, The Netherlands.

[7] J.J.M. Kwaspen, et al, Electronics Letters, 1997, 33, (19), pp. 1657-1658.